CRYSTAL GROWTH & DESIGN

Subscriber access provided by READING UNIV

Article

Effects of supramolecular architecture on halogen bonding between diiodine and heteroaromatic N-oxides

Yakov P. Nizhnik, Alex Sons, Matthias Zeller, and Sergiy V. Rosokha

Cryst. Growth Des., **Just Accepted Manuscript** • DOI: 10.1021/acs.cgd.7b01734 • Publication Date (Web): 10 Jan 2018

Downloaded from http://pubs.acs.org on January 12, 2018

Just Accepted

"Just Accepted" manuscripts have been peer-reviewed and accepted for publication. They are posted online prior to technical editing, formatting for publication and author proofing. The American Chemical Society provides "Just Accepted" as a free service to the research community to expedite the dissemination of scientific material as soon as possible after acceptance. "Just Accepted" manuscripts appear in full in PDF format accompanied by an HTML abstract. "Just Accepted" manuscripts have been fully peer reviewed, but should not be considered the official version of record. They are accessible to all readers and citable by the Digital Object Identifier (DOI®). "Just Accepted" is an optional service offered to authors. Therefore, the "Just Accepted" Web site may not include all articles that will be published in the journal. After a manuscript is technically edited and formatted, it will be removed from the "Just Accepted" Web site and published as an ASAP article. Note that technical editing may introduce minor changes to the manuscript text and/or graphics which could affect content, and all legal disclaimers and ethical guidelines that apply to the journal pertain. ACS cannot be held responsible for errors or consequences arising from the use of information contained in these "Just Accepted" manuscripts.

ACS Publications

Crystal Growth & Design is published by the American Chemical Society. 1155 Sixteenth Street N.W., Washington, DC 20036

Published by American Chemical Society. Copyright © American Chemical Society. However, no copyright claim is made to original U.S. Government works, or works produced by employees of any Commonwealth realm Crown government in the course of their duties.

Effects of supramolecular architecture on halogen bonding between diiodine and heteroaromatic *N*-oxides

Yakov P. Nizhnik,[a] *Alex Sons,*[b] *Matthias Zeller,*[c] *Sergiy V. Rosokha*[b]*

[a] Bioo Scientific, 7050 Burleson Rd, Austin, TX 78744.

[b] Department of Chemistry, Ball State University, Muncie, IN, USA, 47306.

[c] Department of Chemistry, Purdue University, West Lafayette, IN, USA, 47907.

Abstract

Co-crystallization of diiodine with a series of heteroaromatic *N*-oxides produced three types of halogen-bonded associates: a) alternating chains comprising I_2 molecules bridged by oxygen atoms of *N*-oxides of pyridine, quinoline or 4-methylpyridine; b) discrete 2:1 complexes, in which diiodine links a pair of acridine *N*-oxide molecules; and c) amphoteric 1:1 adducts, in which one end of each diiodine molecule is halogen-bonded to *N*-oxide of 4-methoxypyridine or 4-chloroquinoline, and another diiodine's end forms contacts with the other I_2 molecules. In all cases, halogen bonds between diiodine and *N*-oxides are characterized by nearly linear I-I···O angles, close to perpendicular dihedral C-N-O···I angles and N-O···I angles of about 110°. The halogen-bond length in the 1:1 adducts are about 0.3 Å shorter than those in the 2:1 associates and in the infinite chains. Computational analyses confirmed that the variations in I···O separations are related predominantly to the distinct effects of halogen-bond competition in different supramolecular associates. Experimental and computational data also indicated that coordination of the second diiodine to the same oxygen atom of *N*-oxide has a smaller effect on the halogen bond length and energy than coordination of the second *N*-oxide to another iodine atom in the I_2 molecule.

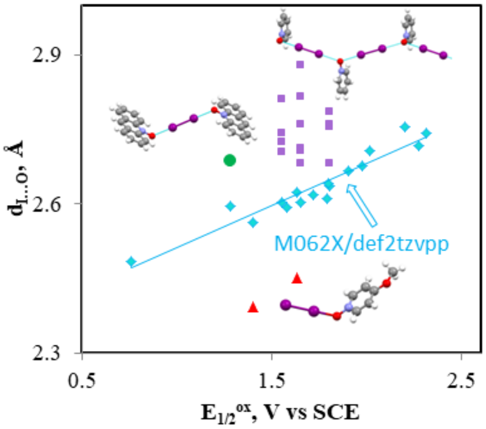

Sergiy V. Rosokha
Ball State University
Chemistry Department
Muncie IN 47306
Phone: 765-285-8615
Fax: 765-285-6505
E-mail: svrosokha@bsu.edu
https://sites.google.com/site/srosokha/

Effects of supramolecular architecture on halogen bonding between diiodine and heteroaromatic *N*-oxides

Yakov P. Nizhnik,[a] *Alex Sons,*[b] *Matthias Zeller,*[c] *Sergiy V. Rosokha*[b]*

[a] Bioo Scientific, 7050 Burleson Rd, Austin, TX 78744.
[b] Department of Chemistry, Ball State University, Muncie, IN, USA, 47306.
[c] Department of Chemistry, Purdue University, West Lafayette, IN, USA, 47907

Abstract

Co-crystallization of diiodine with a series of heteroaromatic *N*-oxides produced three types of halogen-bonded associates: a) alternating chains comprising I_2 molecules bridged by oxygen atoms of *N*-oxides of pyridine, quinoline or 4-methylpyridine; b) discrete 2:1 complexes, in which diiodine links a pair of acridine *N*-oxide molecules; and c) amphoteric 1:1 adducts, in which one end of each diiodine molecule is halogen-bonded to *N*-oxide of 4-methoxypyridine or 4-chloroquinoline, and another diiodine's end forms contacts with the other I_2 molecules. In all cases, halogen bonds between diiodine and *N*-oxides are characterized by nearly linear I-I···O angles, close to perpendicular dihedral C-N-O···I angles and N-O···I angles of about 110°. The halogen-bond length in the 1:1 adducts are about 0.3 Å shorter than those in the 2:1 associates and in the infinite chains. Computational analyses confirmed that the variations in I···O separations are related predominantly to the distinct effects of halogen-bond competition in different supramolecular associates. Experimental and computational data also indicated that coordination of the second diiodine to the same oxygen atom of *N*-oxide has a smaller effect on the halogen bond length and energy than coordination of the second *N*-oxide to another iodine atom in the I_2 molecule.

Introduction

Although halogen bonding became a focus of supramolecular chemistry only during the last two decades, this intermolecular interaction could be identified in the adducts of diiodine with ammonia going back over a century.[1-8] Following seminal UV-Vis studies of the complexes between I_2 and aromatic molecules by Benesi and Hildebrand,[9] and X-ray crystallographic analysis of Br_2 associates with dioxane by Hassel *et al.*,[10] a number of molecular complexes involving halogenated electrophiles were characterized during the 1960s and 1970s.[11-17] Many of these associates (referred to as charge-transfer or donor/acceptor complexes) involved diiodine. In particular, several UV-Vis studies demonstrated that I_2 molecules form strong associates with aliphatic or aromatic *N*-oxides.[14-17] Somewhat later, Kubota *et al.* established the substituent effect on electronic spectra and equilibria constants of a large series of complexes of diiodine with pyridine-*N*-oxides.[18]

Diiodine, the original halogen-bond donor, is capable of forming a variety of associates.[7, 19-22] This diversity is related to the ability of I_2 molecule to simultaneously participate in several halogen bonds in which it can serve both as a halogen-bond donor and acceptor. Based on the extensive analysis of halogen-bonded associates involving dihalogens and interhalogens, Pennington *et al.* pointed out several structural modes of interaction between diiodine and electron donors, B, i.e.: 1) simple adducts, B···I-I; 2) bridged, B···I-I···B; 3) amphoteric, B···I-I···I-I; 4) bridged amphoteric, B···I-I···I-I···I-I···B; and 5) ionic, D^+-I ···· I^- modes.[7] Heteroaromatic *N*-oxides, on the other hand, are excellent halogen-bond acceptors due to the strong nucleophilicity and exceptional steric accessibility of their oxygen atoms in comparison with their parent heterocycles, as well as their ability to form more than one contact with a halogen-bond donor.[23-27] For example, halogen-bonded chains formed by 4,4'-dipyridyl N,N'-dioxide and 1,4-diiodotetrafluorobenzene described in 2001 by Resnati, Metrangolo and co-workers comprised the shortest O···I intermolecular distance (2.75 Å) reported at that moment in the crystallographic literature.[19] More recently, even shorter I-O separations of about 2.3 – 2.4 Å were found by Rissanen *et al.* in the complexes of several *N*-oxides with *N*-iodosuccinimide or *N*-iodosaccharin.[24] Aakeröy and co-workers employed bifurcated halogen bonds between iodofluorobenzenes and *N*-oxides (i.e. bonds in which one oxygen atom participates in two different C-I···O interactions) for the deliberate assembly of molecular polygons in the solid state.[25]

Since the *N*-oxide group stabilizes both Wheland and Meisenheimer complexes, heteroaromatic *N*-oxides are more reactive than their parent heterocycles in both electrophilic and nucleophilic processes.[28, 29] This makes them valuable catalysts, mild nucleophilic oxidants and useful intermediates in synthetic organic chemistry.[29-33] Reactivity of *N*-oxides can be modulated by Lewis and Brønsted-Lowry acids.[34-39] We have shown previously that coordination of the *v*-acceptor, BF_3, to the oxygen atom of the N-O group enhances the π-acceptor strength of 4-nitropyridine- and 4-nitroquinoline *N*-oxides, and the latter form ternary complexes in which *N*-oxide plays a dual role of both Lewis acid and base.[40] The latest publications demonstrated that various reactions of heteroaromatic *N*-oxide can be also catalyzed by diiodine.[31,32]

The ability of heteroaromatic *N*-oxides and diiodine to form strong halogen bonds and the possibility of the use of such bonding in catalysis raise the interest to the structural and electronic features of the complexes comprising these two molecules. The authors of the earlier studies suggested several possible modes of their interactions, such as σ-bonding of diiodine with oxygen or π-bonding with a parallel arrangement of the diiodine molecule above the aromatic ring of *N*-oxide.[41-46] These suggestions, however, were based on the results of NMR, IR and/or UV-Vis measurements. Despite the fact that the discussion of the complexes of diiodine with *N*-oxides has continued for more than 50 years,[14,15,18, 41-46] the definitive elucidation of their structures via X-ray structural analysis is lacking.

Thus, in our current work, we intend to explore the modes of interaction between heteroaromatic *N*-oxides and diiodine. This goal will be achieved via X-ray structural and computational characterization of the association between the diiodine and a series of acridine, quinoline and pyridine *N*-oxides illustrated in Chart 1 (together with their abbreviations).

Chart 1.

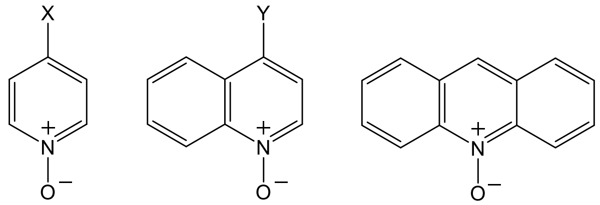

X = H: PyO Y = H: QnO AcrO
X = CH_3: MePyO Y = Cl: ClQnO
X = OCH_3: MeOPyO

Beside clarification of the structural features of the molecular complexes between diiodine and heteroaromatic *N*-oxides, X-ray crystallographic studies of their associates makes it possible to evaluate the effect of the supramolecular architecture on the structural characteristics of halogen bonding. In addition, a variety of potential modes of interactions between diiodine and heteroaromatic *N*-oxides provide vast opportunities for crystal engineering based on the combination of these two molecules.

Results and Discussion

Addition of solid heteroaromatic *N*-oxides to saturated solutions of diiodine in dichloromethane immediately led to a change of color of these solutions from violet to brown (due to the well-known blue shift of the absorption band of I_2 upon its complexation with electron donors[18]). Cooling or slow evaporation of these solutions afforded dark yellow to red-brown crystals of adducts between diiodine and *N*-oxides suitable for single-crystal X-ray measurements (see Experimental section for details). They show three types of halogen-bonded solid-state associates: a) alternating donor/acceptor chains, b) discrete 2:1 complexes, as well as c) 1:1 adducts between heteroaromatic *N*-oxides and diiodines (the latter also show contacts between amphoteric iodine atoms which are not involved in halogen bonding with *N*-oxides).

In particular, when a dichloromethane solution containing equimolar amounts of pyridine-*N*-oxide and diiodine was prepared at room temperature and then cooled down and kept at -60^{o} C for several days, brown crystals were formed. FT-IR measurements of these crystals show that a strong band of the parent

N-oxide around 1250 cm^{-1} (which is related to the N–O stretching vibrations) disappeared and new bands appeared in the 1200-1100 cm^{-1} range (see Figure S1 in the Supporting Information). Such spectral changes were assigned earlier to the complex formation between diiodine and *N*-oxides. [46] X-ray structural analysis of these crystals revealed that they comprise pyridine-*N*-oxide and diiodine in a 1:1 molar ratio. Similar to the diiodine adducts with dioxane reported by Bock,[47] the pyridine *N*-oxides and diiodine moieties form infinite (parallel) alternating chains showing short interatomic I···O contacts (Figure 1, see crystal packing in Figure S2 in the Supporting Information). In the case of *N*-oxides, however, diiodine molecules are linked by bridging oxygen atoms which form two halogen bonds (such coordination was earlier referred to as a bifurcated halogen bond [25]). Geometric characteristics of the halogen bonds in these co-crystals are listed in Table 1.

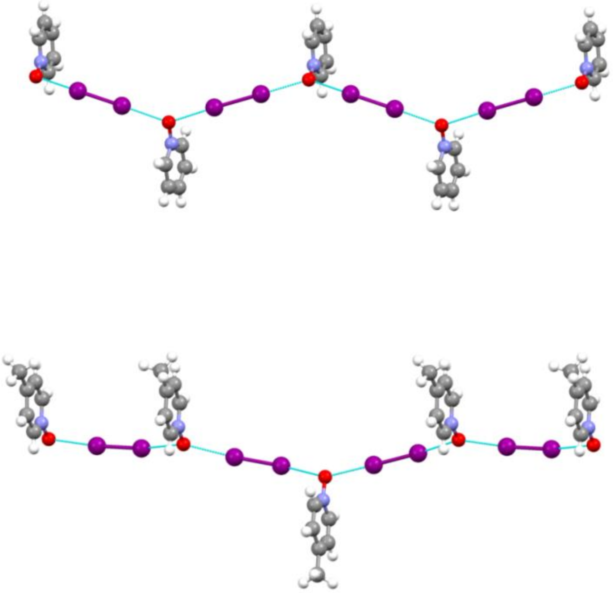

Figure 1. Alternating donor/acceptor chains in the PyO•I_2 (top) and MePyO•I_2 (bottom) co-crystals. Halogen bonds are shown as the light blue lines.

Table 1. Selected bond distances (Å) and angles (°) in the co-crystals of diiodine with *N*-oxides

N-oxide	Type	$d_{I\cdots O}$, Å	I-I…O,°	N-O-I,°	C-N-O-I, °
PyO	Chain	2.684	175.04	109.12	77.91
		2.791	171.46	108.47	88.04
		2.755	173.82	106.70	76.19
		2.754	174.04	106.17	85.40
MePyO	Chain	2.661	174.26	104.43	89.17
		2.874	168.44	106.89	86.85
		2.686	170.66	103.62	83.70
		2.747	168.70	99.56	82.16
		2.698	171.52	107.78	88.04
		2.805	171.99	103.13	89.51
QnO	Chain	2.704	174.16	125.31	77.11
		2.724	177.68	116.30	74.51
		2.743	177.62	114.06	72.59
		2.810	172.58	120.99	72.49
AcrO	2:1	2.686	178.59	118.09	76.19
MeOPyO	1:1	2.393	174.27	113.63	79.60
ClQnO	1:1	2.499	174.34	111.71	63.51

The chains formed by diiodine and pyridine *N*-oxide comprise four crystallographically independent I···O contacts. The interatomic distances between the corresponding oxygen and iodine atoms vary from 2.68 Å to 2.79 Å, i.e., they are about 20-25 % shorter than the sum of the van der Waals radii of oxygen and iodine of 3.50 Å.[48] The I–I···O angles within these pairs are about 171° -175°. Both these characteristics are typical for strong halogen bonds.[4-7] The C-N-O···I dihedral angles in the pyridine *N*-oxide/diiodine pairs are about 80°, and the N-O···I angles in the 106 – 109° range (i.e. the I_2 molecules approach oxygen atoms of *N*-oxides from above of the aromatic rings).

Co-crystals of diiodine with 4-methylpyridine-*N*-oxide comprise very similar donor/acceptor chains (Figure 1 and Figure S2 in the Supporting Information). The geometric characteristics of halogen bonds in this system are also close to that in the PyO•I_2 co-crystals (Table 1). Likewise, co-crystals of diiodine with quinoline *N*-oxide showed chains of alternating halogen-bonded molecules. These interlocked zigzag chains form layers in which stacks of *N*-oxide molecules from four different chains are separated by I_2 molecules (Figure 2).

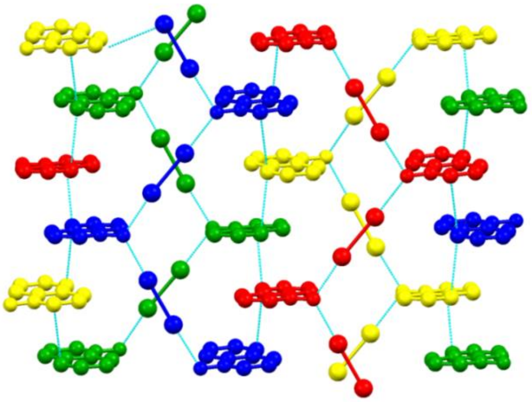

Figure 2. Interlocked zigzag chains in the QnO•I_2 co-crystals. (Note: different colors designate different chains, halogen bonds and short contacts between stacked quinoline *N*-oxide molecules are shown as light blue lines, hydrogen atoms are omitted for clarity).

The angles between the planes of neighboring quinoline *N*-oxide molecules are 2.27 ^{o} and 6.07 ^{o} (i.e. they are almost co-planar). The neighboring molecules are somewhat shifted and turned relatively to each other. For example, the pyridine ring of one molecule overlap with pyridine ring of one of its neighbor, so the distances between centroids of these ring is 3.686Å, and the shortest C…C distances is 3.297 Å. The distance between the phenylene rings of the same molecules is 4.454 Å. In the other, crystallographically independent, neighboring pairs of QnO molecules, pyridine rings are located over phenylene moieties, with the distances between their centroids of 3.765Å and 3.764 Å (and the shortest C…C distances is 3.391 Å). The N-O···I angles in these crystals are somewhat larger than those in the chains formed by diiodine with pyridine *N*-oxide and 4-methylpyridine *N*-oxide (Table 1). The lengths of four crystallographically independent I···O halogen bonds in the QnO•I_2 chains vary in the 2.7 Å – 2.8 Å range, which is essentially the same as that in their PyO•I_2 and MePyO•I_2 analogues.

Co-crystals of diiodine with 4-methoxypyridine and 4-chloroquinoline *N*-oxides show a strikingly different pattern of halogen bonding. In both cases, each I_2 molecule forms only one halogen bond with the oxygen atom of the N-O group, and vice versa (Figure 3). The distance between the oxygen and iodine atoms in the MeOPyO$\cdot I_2$ co-crystals (2.393 Å) is about 32 % shorter than the sum of the van der Waals radii of oxygen and iodine. The distances between the iodine atoms at the other end of the I_2 molecule (i.e. between the iodine atoms which do not form halogen bonds with oxygen) are 3.941 Å. This value is within 0.5 % of their van der Waals separation. In essence, there are no short intermolecular contacts at this diiodine's end.

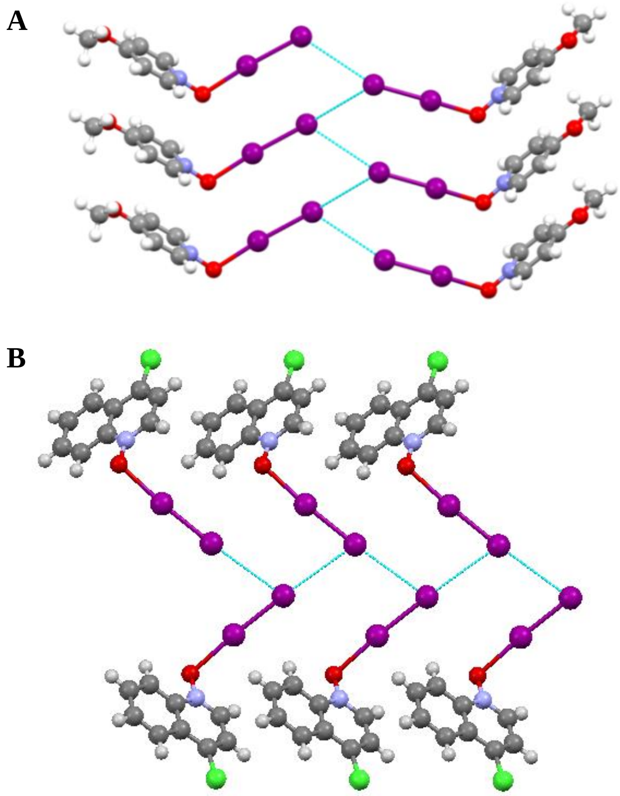

Figure 3. Crystal structures of the 1:1 MeOPyO$\cdot I_2$ (A) and ClQnO$\cdot I_2$ (B) adducts.

The geometric measure of the halogen bond strength, $R_{XY} = d_{X\cdots Y}/(r_X + r_Y)$ (where $d_{X\cdots Y}$ is the separation between the donor and acceptor atoms, X and Y, and r_X and r_Y are their van der Waals radii) for the I$\cdots$O bond in the MeOPyO$\cdot I_2$ co-crystals is 0.683. This value is close to that in the shortest O$\cdots$I halogen bond (R_{XY} = 0.662) found recently by Rissanen *et al.* in the complexes of *N*-iodosaccharin with pyridine-*N*-oxide derivatives.[24] Notably, these very short halogen bonds were observed (in the current study and in Rissanen's work[24]) in the 1:1 donor/acceptor adducts, in which each iodine-containing molecule is halogen-bonded to one *N*-oxide and vice versa. Overall, the distances between oxygen and diiodine in these adducts are much closer to the I-O covalent bond length (~2.05Å) than to the van der Waals separation of oxygen and iodine atoms (3.50 Å).

In the ClQnO·I_2 co-crystals, the O···I bond distance of 2.499 Å (Table 1) is almost as short as in the complexes of diiodine with 4-methoxypyridine *N*-oxide. The contacts between the diiodine ends which are not bonded to the oxygen atoms in these co-crystals are also, at first glance, similar to that in the MeOPyO·I_2 analogues (Figure 3 and Figure S3 in the Supporting Information). Yet, a closer look at the interatomic I···I distances and angles at the diiodine ends which are not halogen-bonded to the oxygen atoms reveals some differences between these two systems. Specifically, in the ClQnO·I_2 co-crystals, the intermolecular I···I separations are 3.860 Å. This value is 4 % shorter than the sum of the van der Waals radii of two iodines. Also, in this case, one I-I···I angle is 175^o yet another angle is 77^o (as compared to 154^o and 118^o in the MeOPyO·I_2 co-crystals). In other words, in the ClQnO·I_2 co-crystals, the top of one iodine forms a rather short contact with the side of another iodine (Figure 3B). Such arrangements (together with the interatomic distances) suggest weak halogen bonding between the iodine atoms in the ClQnO·I_2 co-crystals. Interestingly, these amphoteric iodine atoms participate simultaneously in two halogen bonds. Each iodine serves as a halogen-bond donor in one of the I···I bonds, and it serves as a halogen bond acceptors in another bond. As a result, the iodine molecules form infinite iodine ribbons separated by *N*-oxide molecules (Figure 4, and Figure S3 in the Supporting Information).

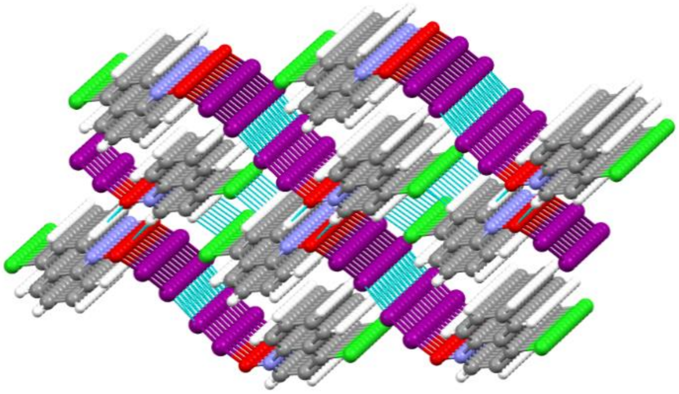

Figure 4. X-ray structure of ClQnO·I_2 showing diiodine ribbons enclosed by the ClQnO molecules.

The halogen-bonding pattern between iodine atoms in the ClQnO·I_2 co-crystals is akin to that observed in the structure of pure diiodine.[49] The unique crystal structure of I_2 (determined as early as 1928) shows the infinite planar 2D-sheets of the halogen-bonded diiodines. Each I_2 molecule within these sheets (in the crystal structure of diiodine) is involved in four halogen bonds , i.e. amphoteric iodine atoms on both sides of diiodine serve simultaneously as halogen-bond donors and acceptors (see Figure S3 in the ESI). In comparison, the diiodine ribbons in the ClQnO·I_2 co-crystals are enclosed by the 4-chloroquinoline *N*-oxides moieties (Figures 3B and 4). As such, they could be considered as the 0.6 nm-wide fragments of the I_2 sheets inside the core formed by the *N*-oxides. The intermolecular I···I distances in the related MeOPyO·I_2 co-crystals are practically the same as their van der Waals separations, and I-I···I orientations deviate much more strongly from the linear and perpendicular angles (*vide supra*). So, despite similarity in the diiodine arrangements (Figure 3), there is hardly any halogen bonding between the diiodines in the MeOPyO·I_2 co-crystals. Still, since the halogen bonds between iodine atoms in the ClQnO·I_2 co-crystals are relatively weak (and the effects of two I···I bonds to one iodine probably somewhat compensate each other due to the dual donor/acceptor role of the iodine atom in these bonds), the I···O distance in the 1:1 adduct of diiodine with 4-chloroquinoline *N*-oxide is close to the corresponding value in the 1:1 MeOPyO·I_2 complex.

Co-crystals of diiodine with acridine-*N*-oxide show another type of halogen-bonded associates. They comprise 2:1 complexes in which an I_2 molecule links two acridine *N*-oxides (Figure 5). As such, they represent an intermediate case between the chains (in which each donor forms bonds with two acceptors and each acceptor forms bonds with two donors) and 1:1 adducts (in which one diiodine is bonded to one *N*-oxide molecule). It is interesting to note, therefore, that the O···I distance in these 2:1

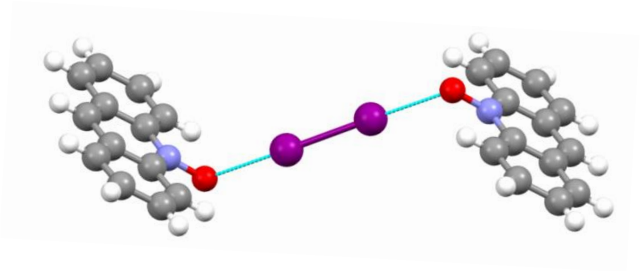

Figure 5. Structure of 2:1 complexes formed by AcrO and I_2 molecules.

complexes (2.686 Å) is close to that in the infinite chains in which each oxygen atom of *N*-oxide and each I_2 are involved in two (bifurcated) halogen bonds (Table 1).

The data in Table 1 indicate that the variations of the I-I···O, N-O···I and C-N-O···I angles in the solid-state associates between diiodine and heteroaromatic *N*-oxides are rather minor. In other words, regardless of the supramolecular architectures, the mutual orientations of the halogen-bonded donor and acceptor are similar. However, the lengths of the halogen bonds differ significantly in the 1:1 adduct from that in the infinite chains and the 2:1 adducts. To verify if such bond-length variations are related to the changes in the type of association (leading to competition of two halogen bonds at the same donor or acceptor), we carried out a computational analysis of the halogen-bonded complexes under study.

DFT (M062X/def2tzvpp) optimizations of the 1:1 *N*-oxide/I_2 pairs produced structures in which mutual donor/acceptor arrangements were similar to those measured in the solid state associates, as illustrated for the diiodine adduct with 4-methylpyridine *N*-oxide in Figure 6. In the experimental and calculated MePyO·I_2 complexes, the diiodine molecule is halogen-bonded to the oxygen atom of the *N*-oxide. The N-O···I angles vary from 99 ^{o} to 106^{o} in the crystallographically independent solid-state MePyO·I_2 associates, and this value is 106^{o} in the calculated complex. The dihedral C-N-O···I angles vary from 83^{o} to 89^{o} in the solid state complexes, and the value of the corresponding angle in the calculated structure is essentially 90^{o}. However, the halogen bond length in the calculated 1:1 dyad (2.604 Å) is about 0.15 Å shorter than the average I···O distance in the solid-state chains formed by the I_2 molecules and 4-methylpyridine *N*-oxides (Table 1).

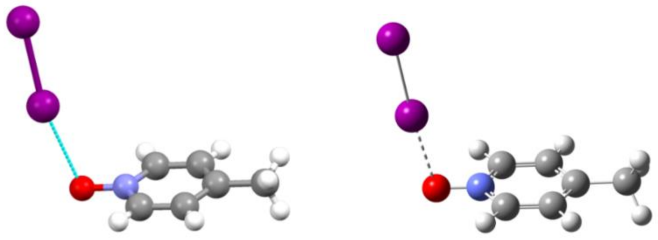

Figure 6. Structures of the MePyO·I_2 complexes from X-ray analysis (left) and from computations (right).

Interaction energies and geometric characteristics of the calculated 1:1 complexes between diiodine and the heteroaromatic *N*-oxides are listed in Table 2. All calculated complexes show strong halogen bonding, with the interactions energies varying from about -8.6 kcal/mol to -10.0 kcal/mol. The I-I···O angles in these complexes are close to 180°, N-O···I angles are about 108° and dihedral C-N-O···I angles are mostly close to 90°. These angles are similar to the corresponding values measured in the solid-state associates (Table 1), which confirms that the M062X/def2tzvpp computations reproduce very well the mutual arrangements of the donor and acceptor in the halogen-bonded complexes.

Table 2. Interaction energies (ΔE) and selected geometric characteristic of the diiodine complexes with heteroaromatic *N*-oxides.

	ΔE, kcal/mol[c]	$d_{I\cdots O}$, Å	N-O-I,°	I-I···O,°	C-N-O-I, °
PyO	-8.70	2.637	110.4	176.0	62.6
MePyO	-9.33	2.604	105.8	175.5	89.7
QnO	-8.93	2.603	108.8	177.1	66.7
ClQnO	-8.62	2.624	107.9	175.9	89.4
MeOPyO	-10.04	2.562	107.3	175.8	81.1
AcrO	-9.47	2.596	107.9	178.0	89.4

a) From M062X/def2tzvpp computations. b) $\Delta E = E_{comp} - (E_{NO} + E_{I2}) + BSSE$, where E_{comp}, E_{NO} and E_{I2} are sums of the electronic and zero-point energies of the complex, *N*-oxide and I_2 and BSSE is a basis set superposition error.

Comparison of the ΔE and $d_{I\cdots O}$ values in Table 2 indicates that changes in the calculated I···O distances for different *N*-oxides generally follow the variations of the interaction energy (i.e., the complexes with more negative ΔE are characterized by shorter halogen bonds). A closer inspection of these variations suggests that they are related to the strength of the electron donors. Quantitatively, the latter can be expressed via their oxidation potentials, $E_{1/2}^{ox}$. The values of $E_{1/2}^{ox}$ obtained from electrochemical measurements of a number of heteroaromatic *N*-oxides were reported earlier.[50,51] Together with the data from Table 2, they allow to check the relationship between $d_{I..O}$ and $E_{1/2}^{ox}$. However, the $E_{1/2}^{ox}$ values of the *N*-oxides under study and the calculated I···O separations in their complexes with diiodine vary within a fairly narrow ranges of $E_{1/2}^{ox} = 1.6 \pm 0.2$ V vs SCE and $d_{I\cdots O} = 2.60 \pm 0.04$ Å (see Table 2 and Table S2 in the Supporting Information). Thus, to verify the relationship between $d_{I..O}$ and $E_{1/2}^{ox}$ in a wider range, we carried out M062X/def2tzvpp computations of the halogen-bonded complexes of diiodine with an extended series of heteroaromatic *N*-oxides. As illustrated in Figure 7, the halogen-bond lengths,

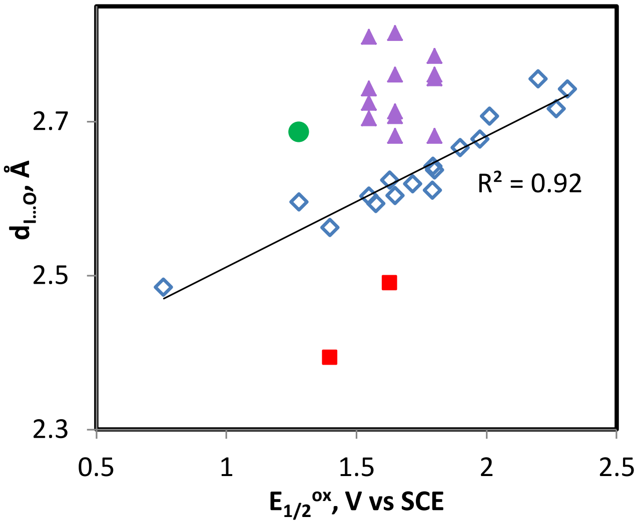

Figure 7. Relationship between $E_{1/2}^{ox}$ of heteroaromatic *N*-oxides and $d_{I\cdots O}$ in the calculated 1:1 complexes, (◊), as well as in the solid-state 1:1 adducts (■), 2:1 complex (●) and infinite chains (▲). (See Table S2 in the Supporting Information for the $E_{1/2}^{ox}$ values and $d_{I..O}$ in the calculated complexes).

$d_{I\cdots O}$, within these calculated complexes show a rather strong correlation ($R^2 = 0.92$) with the oxidation potentials of the heteroaromatic *N*-oxides.[52] This figure also demonstrates that the $d_{I\cdots O}$ values for 1:1 adducts obtained from the X-ray measurements of the MeOPyO·I_2 and ClQnO·I_2 co-crystals are located far below the calculated trend line. The $d_{I\cdots O}$ values measured experimentally for the (solid-state) infinite chains and 2:1 complex are located above the calculated trend line.

It should be mentioned that the crystallographically non-equivalent I···O contacts in the infinite chains formed by diiodine with PyO, MePyO or QnO molecules vary within rather large ranges (0.1 Å - 0.2 Å). Such variations of the experimental halogen-bond length are probably related to the very shallow minima in the dependencies of energies of the complexes on intermolecular separations. As illustrated for the complex between 4-methylpyridine *N*-oxide and diiodine in Figure 8, the increase or decrease of $d_{I\cdots O}$ by about 0.1 Å from its optimal value (corresponding to the global minimum) is accompanied by an energy change of only 0.25 kcal/mol. As such, in the solid state,

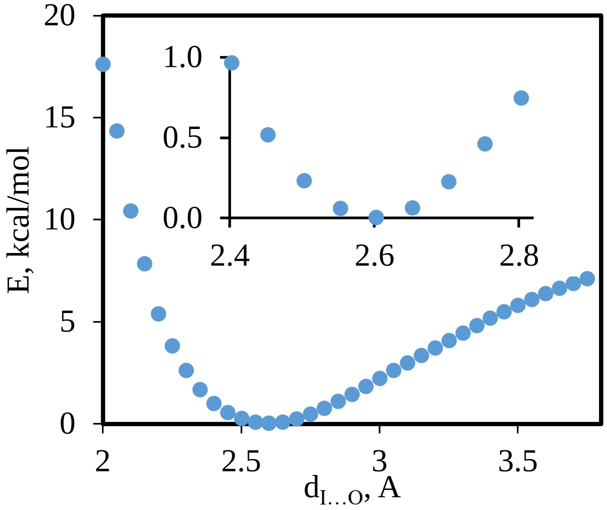

Figure 8. Dependence of the energy of halogen bonded complexes on the I···O distance relative to the energy of the fully-optimized complex. Insert: variation of the energy near the minimum.

this halogen bond length can be easily adjusted by crystal forces. Most importantly, the difference between the halogen bond lengths in the 1:1 adducts (squares in Figure 7), and those in the 2:1 complex (circle) and in the infinite chains (triangles), is substantially larger than the variations of $d_{I\cdots O}$ within one type of supramolecular complex. Furthermore, this large distinction between the $d_{I\cdots O}$ values for different modes apparently is not related to the oxidation potentials of *N*-oxides or to the values of the most negative potential on the surface of the *N*-oxides or the energies of their HOMOs (see Figure S4 in the Supporting Information[52]). For example, the oxidation potential of 4-chloroquinoline *N*-oxide is slightly higher (i.e., it is a weaker donor) than that of quinoline *N*-oxide (Table S2). Yet, the halogen-bond length in the 1:1 adduct formed by 4-chloroquinoline *N*-oxide is about 0.3 Å shorter than the $d_{I\cdots O}$ measured in the chains formed by diiodine with quinoline *N*-oxide. In fact, the difference between the average bond length in the infinite chains and that measured in the 1:1 complexes is larger than the limiting $d_{I\cdots O}$ values in the calculated complexes (despite more than 1.5 V difference in the $E_{1/2}^{ox}$ of the corresponding *N*-oxides). In other words, the halogen bonding of diiodine with the second *N*-oxide molecules has more pronounced effect on the halogen-bond length than the changes in the electron-donor strength of *N*-oxide. This supports the conclusion that such differences are related primarily to the changes in the mode of supramolecular donor/acceptor interaction (1:1 adduct vs 2:1 complexes or alternating chains).

The values of $d_{I\cdots O}$ are definitely expected to change with variations of $E_{1/2}^{ox}$ (or V_{min}), as indicated by the dependences in the calculated values in Figure 8 and Figure S4 in the Supporting Information. However, in order to verify these relationships experimentally, it is necessary to establish variations of such bonds within the same mode of association. Furthermore, to draw reliable conclusions, an analysis of structural data for a wider series of *N*-oxides is needed (including much weaker and stronger electron donors, e.g. 4-nitropyridine *N*-oxide and 4-dimethylaminopyridine *N*-oxide).[53]

It is also noticeable that the experimental halogen-bond length in the 2:1 acridine *N*-oxide/diiodine complex (in which I_2 is bonded to two oxygen atoms, but the latter participate in only one halogen bond) is much longer than that in the 1:1 complexes. (Similar differences in halogen bond length in 2:1 and 1:1 complexes of 1,3-diiodo-5,5-dimethylhydantoin were reported recently by Fourmigue *et al.* [54]) In fact, the I···O distance of 2.686 Å in the 2:1 complex of AcrO with I_2 is almost the same as the $d_{I\cdots O}$ values in the infinite chains in which each diiodine and each oxygen atom participates in two halogen bonds. This suggests that the elongation of intermolecular distances in the infinite chains as compared to that in the 1:1 adducts is related mostly to the competition of two halogen bonds at the same diiodine molecule. This suggestion is supported by the results of the calculations on the 2:1 and 1:2 complexes between pyridine *N*-oxide and diiodine. The energies and intermolecular distances in these complexes, as well as in the corresponding 1:1 dyad are shown in Figure 9.

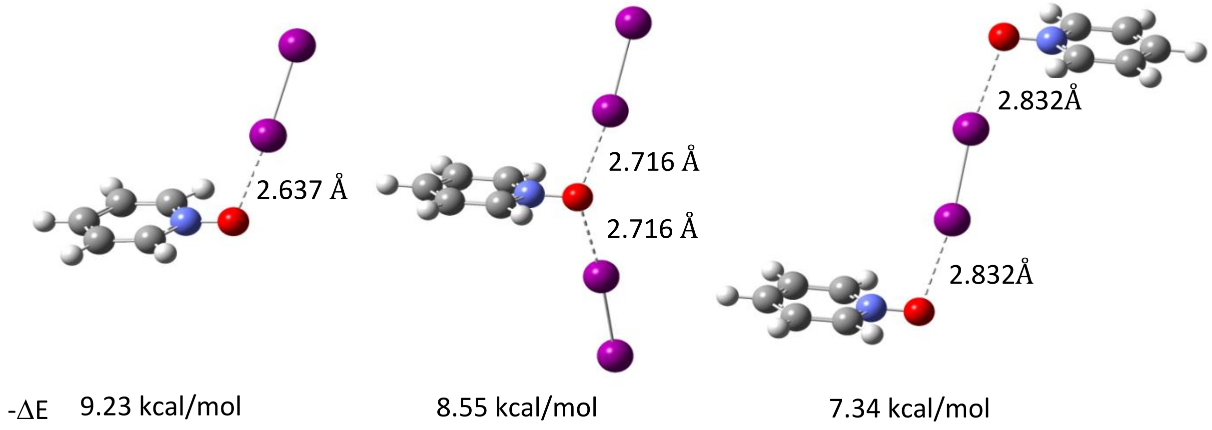

Figure 9. Interaction energies (per one halogen bond) and I···O distances in the 1:1. 1:2 and 2:1 complexes between PyO and I_2 molecules (from M062X/def2tzvpp computations).

Figure 9 demonstrates that bonding of two I_2 molecules to one oxygen atom decreases the energy of each halogen bond by about 0.7 kcal/mol as compared to that in the 1:1 complex. However, if two *N*-oxides are bonded to one diiodine, the energy of each bond is decreased by about 1.9 kcal/mol (i.e. the difference is almost three times larger). The changes of the bond lengths follow the trend observed in the changes of energies. Specifically, bonding of two diiodines to one oxygen atom of an *N*-oxide leads to an increase of halogen bond length by about 0.079 Å. In comparison, bonding of two *N*-oxides to one diiodine results in an increase of the bond length by 0.195 Å. Thus, both experimental and computational data indicate that coordination of a second diiodine to the same oxygen atom of an *N*-oxide has a smaller effect than coordination of the second *N*-oxide to another iodine atom of the I_2 molecule.

To clarify the reason for these differences, we calculated the effects of the coordination of diiodine to a heteroaromatic *N*-oxide on the properties of both interacting molecules. Within the framework of the electrostatic (σ-hole) model,[4-6, 55] halogen bonding between these two molecules is related to the attraction of a σ-hole on the surface of the I_2 molecule to the area of negative potential on the surface of the oxygen atom of the *N*-oxide, as illustrated in Figure 10 (left).

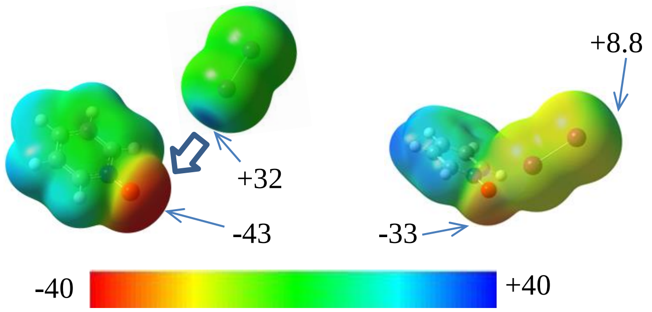

Figure 10. ESPs of PyO, diiodine and their halogen-bonded complex (numbers show values of ESP in kcal/mol, see Figure S5 in ESI for additional views of the ESPs of the complex and its components).

The coordination of diiodine to *N*-oxide results in polarization of both halogen-bonded molecules. Accordingly, the σ-hole on the non-coordinated iodine atom is characterized by a much lower value of maximum positive potential $V_{max} = 8.8$ kcal/mol, as compared to $V_{max} = 32.1$ kcal/mol, calculated for the free I_2 molecule. On the other hand, pyridine *N*-oxide shows the most negative potential $V_{min} = - 43.0$ kcal/mol on the surface of the oxygen atom. Coordination of the diiodine molecule changes this value to -

33.2 kcal/mol. So, halogen bonding between diiodine and *N*-oxide is accompanied by a much more pronounced modification of the V_{max} value on the other end of the I_2 molecule than the change of V_{min} on the surface of the oxygen atom of *N*-oxide (participating in this halogen bonding). Therefore, halogen bonding of the second *N*-oxide to halogen-bonded diiodine is affected by the first halogen bond more substantially than coordination of the second diiodine to the same oxygen atom of *N*-oxide.

While consideration of the ESP surfaces allows for explaining variations of the $d_{I\cdots O}$ with the change of the stoichiometry, it overlooks the question of the donor/acceptor arrangements in their complexes. In particular, the most negative potentials on the surfaces of the *N*-oxide under study are observed on the top of the oxygen atoms along the extension of the N-O covalent bonds. Thus, to maximize electrostatic attraction, the diiodine is expected to approach the oxygen along the N-O bond (resulting in an N-O···I angle of about 180^o). Yet, the experimental and calculated complexes are characterized by an N-O···I angle of about 110^o regardless of the nature of *N*-oxide or mode of interaction. Similar (roughly tetrahedral) angles were observed earlier in the halogen-bonded complexes of iodinated molecules with selenides, and they were related to the electron-pair donation from the HOMO of selenium to the LUMO of iodine.[56] Consideration of molecular-orbital shapes of heteroaromatic *N*-oxides and diiodine together with the geometries of their complexes (as illustrated for $MePyO \cdot I_2$ in Figure 11) suggests that analogous HOMO/LUMO interactions play a significant role in the halogen bonding of these molecules.[57-59] The changes in the bond-length in the 2:1 and 1:2 complexes in this case can be related to the larger effect of halogen bonding on the LUMO of diiodine than on the HOMO of the *N*-oxide (Table S3 in the Supporting Information).

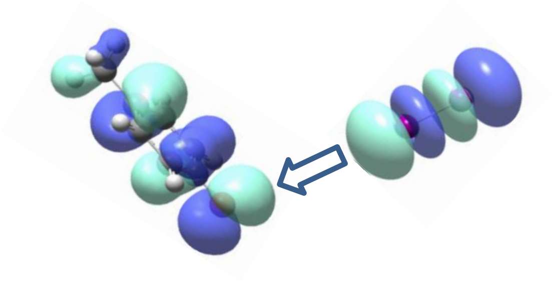

Figure 11. Frontier (HOMO/LUMO) orbital shapes of 4-methylpyridine-*N*-oxide and diiodine and their role in formation of the halogen-bonded complex.

Conclusion.

X-ray crystallographic and computational analyses established three major types of halogen-bonded associates between heteroaromatic *N*-oxides and diiodine, i.e., infinite donor/acceptor chains, 2:1 associates in which I_2 molecule links two *N*-oxide molecules and (more or less isolated) 1:1 adducts between *N*-oxides and diiodines. Regardless of the supramolecular architecture of the co-crystals, the relative orientations of the halogen-bonded donors and acceptors are similar. However, the interatomic I···O distances in the 1:1 adducts are ~0.3 Å shorter compared to that in the 2:1 associates or infinite chains. These distinctions are related to the competition of two I···O halogen bonds, and the fact that the effects of coordination of two *N*-oxides at the opposite ends of I_2 molecule are more pronounced than that of diiodines coordinated to the same (bridging) oxygen atom.

In general, the variations of the bond lengths in various types of supramolecular complexes (resulted from cooperation or competition of co-existing intermolecular interactions [60-66]) are not surprising. For example, structural characteristics of the extensive series of halogen-bonded complexes of dihalogens and interhalogens, which were reviewed by Pennington *et al.*[7], indicate that halogen-bond lengths in the 1:1 adducts are usually shorter than the separations between analogous atoms in infinite donor/acceptor chains. However, the earlier examples of such variations were focused on one reactant or involved significant changes in the nature of halogen-bond donor or acceptor or type of halogen bonding.[7,54,60-66] In comparison, the current work provides examples of the changes in bond length in mono- and ditopic bonding of both halogen bond donors and acceptors in 1:1, 2:1 associates and infinite chains formed by diiodine with the analogous *N*-oxides. Moreover, we have shown that while the calculated halogen-bond lengths are related to the strength of the electron donors, the changes of supramolecular architectures have more pronounced effects on intermolecular separations in the solid-state adducts. It thus underscores the importance of accounting for variations in supramolecular architectures in comparison of intermolecular bond lengths obtained from the solid-state measurements, as well as in their correlations with the data from solution, gas-phase or computational studies.

Experimental Section

Materials. Commercially available PyO, MePyO, MeOPyO, QnO and 4-nitroquinoline *N*-oxide were used without additional purification. ClQnO was prepared by the reaction of 4-nitroquinoline *N*-oxide with HCl.[67] AcrO was prepared by the oxidation of acridine by peroxobenzoic acid in CH_2Cl_2 and purified using flash chromatography on silica gel (eluent CH_2Cl_2:MeOH 10:1), following recrystallization from an ethanol-water (2:1) solution and subsequent drying in a desiccator over P_2O_5 for a week.[68]

Co-crystals of diiodine with various *N*-oxides were prepared by cooling or slow evaporation of dichloromethane solutions containing 1:1 molar ratios of both components. In particular, to prepare adducts with PyO, MePyO and ClQnO, diiodine (102 mg, 0.40 mmol) was dissolved in 4 mL of anhydrous dichloromethane and the equivalent amounts (0.40 mmol) of the corresponding *N*-oxides were added to these solutions. After the starting materials were dissolved, the solutions were kept at -30^{o}C for one day and then at -60^{o}C for two days. This resulted in the formation of crystals suitable for X-ray structural measurements. To prepare co-crystals of diiodine with AcrO, QnO and MeOPyO, the dichloromethane solutions containing analogous amounts of components were slowly evaporated in a desiccator in the presence of mineral oil.

Single crystals of diiodine with MeOPyO, AcrO, and QnO were coated with mineral or Fomblin oil and quickly transferred to the goniometer head of a Bruker Quest diffractometer with a fixed chi angle and a molybdenum radiation sealed tube fine focus X-ray tube (λ = 0.71073 Å). Intensity data for X-ray crystallographic analysis of diiodine associates with PyO, MePyO and ClQnO were collected at 173 K with a Bruker SMART Apex diffractometer equipped with a CCD detector using Mo Kα radiation (λ= 0.71073 Å). Reflections were indexed and processed, and the files were scaled and corrected for absorption using APEX3.[69] The space groups were assigned and the structures were solved by direct methods using XPREP within the SHELXTL suite of programs[70] and refined by full matrix least squares against F^2 with all reflections using Shelxl2016[71] using the graphical interface Shelxle.[72] If not specified otherwise, H atoms attached to carbon and nitrogen atoms and hydroxyl hydrogens were positioned geometrically and constrained to ride on their parent atoms, with C-H bond distances of 0.95 Å for aromatic and C-H, 1.00, 0.99 and 0.98 Å for aliphatic C-H, CH_2 and CH_3 moieties, respectively. Methyl H atoms were allowed to rotate but not to tip to best fit the experimental electron density. $U_{iso}(H)$ values were set to a multiple of $U_{eq}(C)$ with 1.5 for CH_3, and 1.2 for C-H units, respectively. Crystallographic, data collection and refinement details are listed in Table 3. Complete crystallographic data, in CIF format, have been deposited with the Cambridge Crystallographic Data Centre. CCDC 1588334-1588339 contain the supplementary crystallographic data for this paper. These data can be obtained free of charge via www.ccdc.cam.ac.uk/data_request/cif.

Table 3. Crystallographic, data collection and structure refinement details

	MeOPyO·I_2	QnO·I_2	AcrO·I_2	PyO·I_2	MePyO·I_2	ClQnO·I_2
Chem. formula	$C_6H_7NO_2\cdot I_2$	$C_9H_7NO\cdot I_2$	$2(C_{13}H_9NO)\cdot I_2$	$C_5H_5NO\cdot I_2$	$C_6H_7NO\cdot I_2$	$C_9H_6ClNO\cdot I_2$
M_r	378.93	398.96	644.22	348.9	362.93	433.40
Cryst. system	Monoclinic	Monoclinic	Monoclinic	Triclinic	Triclinic	Monoclinic
Space group	$P2_1/c$	$P2_1/c$	$P2_1/c$	$P\bar{1}$	$P\bar{1}$	$P2_1$
a (Å)	12.5018 (8)	10.5555 (6)	7.1316 (10)	9.132(5)	9.6417(14)	9.762(2)
b (Å)	4.2736 (3)	15.4203 (8)	11.1071 (16)	9.374(5)	10.9728(17)	6.1078(15)
c (Å)	18.8796 (12)	13.7263 (7)	14.426 (2)	10.755(6)	14.931(3)	10.743(3)
α (°)	90.00	90.00	90.00	91.833(10)	68.470(3)	90.00
β (°)	108.5094 (17)	104.715 (2)	101.547 (5)	90.119(10)	88.067(5)	116.064(4)
γ (°)	90.00	90.00	90.00	107.266(9)	86.905(3)	90.00
V (Å^3)	956.52 (11)	2160.9 (2)	1119.6 (3)	878.7(8)	1467.1(4)	575.4(4)
Z	4	8	2	4	6	2
T, K	150	150	150	173	173	173
μ (mm^{-1})	6.53	5.78	2.84	7.09	6.37	5.99
n measd	27011	34754	18241	9486	18523	4093
n indpt	3654	6538	4044	4971	8505	2799
n obs [$I > 2\sigma(I)$]	3416	4847	3303	3467	6741	2637
R [$F^2 > 2\sigma(F^2)$]	0.021	0.047	0.025	0.062	0.036	0.035
$wR(F^2)$	0.046	0.114	0.054	0.177	0.087	0.092
S	1.25	1.07	1.09	1.07	0.99	1.05
CCDC	1588338	1588339	1588337	1588335	1588336	1588334

Computations. Quantum-mechanical calculations were carried out using the Gaussian 09 suite of programs.[73] Geometries of *N*-oxides, diiodine and halogen-bonded complexes were optimized in the gas phase via DFT calculations with the M06-2X functional and the def-TZVPP basis set.[74] To obtain fully-optimized complexes, geometry optimizations were carried out without constraints using the default convergence criteria for Gaussian 09. The absence of imaginary frequencies confirmed that the optimized structures represent true minima. Dependence of the energies of the halogen-bonded complexes on $d_{I\cdots O}$ was obtained via constrained optimization with the fixed I···O distances. The energies of interaction for all dyads were determined as: $\Delta E = E_{comp} - (E_{NO} + E_{I2}) + BSSE$, where E_{comp}, E_{NO} and E_{I2} are sums of the electronic and ZPE of the complex, *N*-oxide and I_2, and BSSE is a basis set superposition error.[75] Frontier orbital shapes were evaluated at 0.02 isovalues and electrostatic potentials were calculated on the 0.001 electrons bohr^{-3} molecular surfaces. Energies and atomic coordinates of the calculated complexes are listed in the Supporting Information.

Acknowledgements. We thank the National Science Foundation for the financial support of this work (grant CHE-1607746). We also thank W. Borley for the assistance in the analysis of computational data, J.J. Lu for the assistance in the X-ray measurements of PyO•I_2, MePyO•I_2 and ClQnO•I_2, and the R. A. Welch Foundation for the financial support of these measurements. X-ray structural measurements of QnO·I_2, MeOPyO·I_2, and AcrO·I_2 were supported by the National Science Foundation through the Major Research Instrumentation Program under Grant No. CHE 1625543 (funding for the single crystal X-ray diffractometer).

Supporting Information. FT-IR spectra of adducts (Figure S1), crystal packing of PyO•I_2 and MePyO•I_2 (Figure S2), diiodine ribbons in MeOPyO·I_2, ClQnO·I_2 and I_2 crystals (Figure S3); correlation between $d_{I\cdots O}$ and V_{min} or E(HOMO of *N*-oxides (Figure S4), ESP surfaces of PyO, diiodine and their halogen-bonded complex (Figure S5), calculated energies of adducts and their components (Table S1), $E_{1/2}^{ox}$, V_{min} and E(HOMO) of *N*-oxides and $d_{I\cdots O}$ in their complexes (Table S2), effect of halogen bonding on HOMO/LUMO energies (Table S3), atomic coordinates of calculated complexes.

References and Notes.

1. Colin, J. J. *Ann. Chim.* **1814**, *91*, 252–272.

2. Guthrie, F. *J. Chem. Soc.* **1863,** *16*, 239 – 244.

3. Farina, A.; Meille, S.V.; Messina, T., Metrangolo, P.; Resnati, G.; Vecchio, G. *Angew. Chem. Int. Ed.* **1999**, *38*, 2433-2436.

4. Legon, A.C. *Angew. Chem. Int. Ed.* **1999**, *38*, 2687-714.

5. Metrangolo, P.; Resnati, G. *Chem. Eur. J.* **2001**, *7*, 2511-2519.

6. Cavallo, G.; Metrangolo, P.; Milani, R.; Pilati, T.; Priimagi, A.; Resnati, G.; Terraneo, G. *Chem. Rev.* **2016**, *16*, 2478-2601.

7. Pennington, W. T.; Hanks, T.W.; Arman, H. D. *Struct. Bond.* **2008**, *126*, 65-104.

8. Gilday, L.; Robinson, S.; Barendt, T.; Langton, M.; Mullaney, B.; Beer, P. *Chem. Rev.* **2015**, *115*, 7118-7195.

9. Benesi, H. A.; Hildebrand; J. H. *J. Am. Chem. Soc.* **1949**, *71*, 2703-2707.

10. Hassel, O.; Hvoslef, J. *Acta Chem. Scand*. **1954**, *8*, 873.

11. Andrews, L.J.; Keefer, R.M. *Molecular Complexes in Organic Chemistry*; Holden-Day: San-Francisco, 1964.

12. Bent, H.A. *Chem. Rev.* **1968,** *68, 587-648.*

13. Mulliken, R.S.; Person, W. B. *Molecular Complexes*; Wiley: N.Y. 1969.

14. Kubota T.; Yamakawa M.; Takasuka M.; Iwatani K.; Akazawa H.; Tanaka I. J. *Phys. Chem*. **1967**, *71*, 3597-3604.

15. Kubota T. *J. Am. Chem. Soc.* **1965**, *87*, 458-468.

16. Kulevsky, N.; Severson, R.G. Jr. *Spectrochim. Acta*. **1970**, *26A*, 2227-2228.

17. Kulevsky, N.; Severson, R. G. Jr. *J. Phys. Chem.* **1971**, *75*, 2504-2506.

18. Uno B.; Kano K.; Kaida N.; Kubota T. *Spectrochim. Acta.* **1989**. *45A*, 937-943.

19. Walsh, R. B.; Padgett, C. W.; Metrangolo, P.; Resnati, G.; Hanks, T. W.; Pennington, W. T. *Cryst. Growth Des.* **2001**, *1*, 165-175.

20. Rimmer, E. L.; Bailey, R. D.; Hanks, T. W.; Pennington, W. T. *Chem. Eur. J.* 2000, *6*, 4071-4081.

21. Schuster, I. I.; Roberts J. D. *J. Org. Chem.* **1979**, *44*, 2659-2662.

22. Aronson, S.; Epstein, P.; Aronson, D. B.; Wieder, G. *J. Phys. Chem.* **1982**, *86*, 1035-1037.

23. Messina, M. T.; Metrangolo, P.; Panzeri, W.; Pilati, T.; Resnati, G. *Tetrahedron* **2001**, *57*, 8543-8550.

24. Ruttreddy, R.; Jurcek, O.; Bhowmik, S.; Makela, T.; Rissanen, K. *Chem. Commun.* **2016,** *52, 2338-2341*.

25. Aakeröy, C. B.; Wijethunga, T.K.; Desper, J. *CrystEngComm*. **2014,** *16*, *28-31*.

26. Puttreddy, R.; Topic, F.; Valkonen, A.; Rissanen, K. *Crystals* **2017**, *7*, 214/1-214/11.

27. Topic, F.; Puttreddy, R.; Rautiainen, J. M.; Tuononen, H. M.; Rissanen, K. *CrystEngComm*. **2017**, *19*, 4960-4963.

28. Ochiai E. *Aromatic Amine Oxides;* Elsevier: Amsterdam, 1967.

29. Albini A.; Pietra S. *Heterocyclic N-Oxides;* CRC Press: Boca Raton, Ann Arbor, Boston, 1991.

30. Wang, Y.; Zhang, L. *Synthesis* **2015**, *47*, 289-305.

31. Zhang, Z.; Pi, C.; Tong, H.; Cui, X.; Wu, Y. *Org. Lett.* **2017**, *19*, 440-443.

32. Sumunnee, L; Buathongjan, C.; Pimpasri, C.; Yotphan, S. *Eur. J. Org. Chem.* **2017,** *2017*, 1025-1032 .

33. Fu, W.-K.; Sun, K.; Qu, C.; Chen, X.-L.; Qu, L.-B.; Bi, W.-Z.; Zhao, Y.-F. *Asian J. Org. Chem*. **2017**, *6*, 492-495.

34. Ochiai E. *J. Org. Chem.* **1953**, *18*, 534.

35. Ryzhakov A. V.; Vapirov V. V.; Rodina L. L. *Russ. J. Org. Chem.* **1991**, *27*, 955-959.

36. Ryzhakov A. V.; Rodina L. L. *Russ. J. Org. Chem*. **1994**, 30, 1417-1420.

37. Ryzhakov A.V.; Alekseeva O. O.; Rodina L. L. *Russ. J. Org. Chem.* **1994**, *30*, 1411-1413.

38. Andreev V. P.; Ryzhakov A. V. *Chem. Heterocycl. Comp.* **1999**, 1443-1461.

39. Andreev V. P.; Nizhnik Y. P. *Russ. J. Org. Chem*. **2001**, 37, 148-150.

40. Nizhnik, Y. P.; Lu, J. J.; Rosokha, S. V.; Kochi, J. K. *New J. Chem.* **2009**, *33*, 2317-2325.

41. Ryzahkov, A. V.; Nizhnik, Y. P.; Andreev, V. P. *Russ. J. Org. Chem.* **2000**, *36*, 918-920.

42. Sobczyk, A. L.; Dannel, J.; *J. Chem. Soc., Faraday Trans*, **1972**, *1*, 1544-1549.

43. Ryzhakov A.V.; Andreev V.P.; Rodina L.L. *Russ. J. Org. Chem.* **1998**, *34*, 549-551.

44. Ponomarenko, S. P.; Borovikov, Yu. Ya.; Sivachek, T. E.; Makovetskii, V. P. *Russ. J. Gen. Chem.* **2004**, *74*, 1936 -1942.

45. Ponomarenko, S. P.; Borovikov, Yu. Ya.; Sivachek, T. E.; Vovk, D. N. *Russ. J. Gen. Chem.* **2005**, *75*, 181-185.

46. Kubota, T.; Ezumi, K.; Yamakawa, M.; Matsui Y. *J. Mol. Spectr.* **1967**, *24*, 378-379.

47. Bock, H.; Holl, S. *Z. Naturforsch. B* **2001**, *56*, 111.

48. Bondi, A. *J. Phys. Chem.* **1964**, *68*, 441-451.

49. Harris, P M; Mack, E; Blake, F. C. *J. Am. Chem. Soc.* **1928**, *50*, 1583-1600.

50. Kubota, T.; Nishilkida, K.; Miyazaki, H.; Iwatani, K.; Oishi, Y. *J. Am. Chem. Soc.* **1968**, *90*, 5080-5090.

51. Koldasheva, E. M.; Geletiy, Y. V.; Yanilkin, V. V. Strelec, V. V. *Izv. Akad. Nauk SSSR. Ser. Khim.* **1990**, 994-999.

52. Since the most negative potential on the surfaces of N-oxides, V_{min}, or energy of their HOMO, are correlated with the values of $E_{1/2}^{ox}$, the interatomic I···O distances show similar correlations with V_{min} or E_{HOMO} (with R^2 =0.88 in both cases, see Table S2 and Figure S4 in the Supporting Information). Most importantly, the experimental I···O distances in the 1:1 adducts are arranged below, and in 2:1 complexes and in chains are observed above the trend lines in all these correlations.

53. Up to now, however, our effort to crystallize co-crystals of such N-oxides with diiodine were unsuccessful (they produced crystals of products of redox reactions).

54. Nicolas, I.; Barriere, F.; Jeannin, O.; Fourmigue, M.; *Cryst. Growth Des.* **2016**, *16*, 2963-2971.

55. Politzer, P.; Murray, J. S.; Clark, T. *Phys. Chem. Chem. Phys.* **2010**, *12*, 7748-7757.

56. Arman, H. D.; Rafferty, E. R.; Bayse, C. A. Pennington, W. T. *Cryst. Growth Des.* **2012**, *12*, 4315-4323.

57. Rosokha, S. V.; Stern, C. L.; Swartz, A.; Stewart, R. *Phys. Chem. Chem. Phys.* **2014**, *16*, 12968-12979.

58. Rosokha S.; Vinakos, M. *Cryst. Growth Des.* **2012**, *12*, 4149-4156.

59. It should be stressed, however, that the role of electrostatics and weakly-covalent (molecular-orbital) interactions in the halogen bonding of heteroaromatic N-oxides with diiodine is beyond the scope of the current work and their clarification requires a separate study.

60. Berger, G.; Robeyns, K.; Soubhye, J.; Wintjens, R.; Meyer, F. *CrystEngComm* **2016**, *18*, 683–690.

61. Lu, Y.; Liu, Y.; Li, H.; Zhu, X.; Liu, H.; Zhu,W. *J. Phys. Chem. A* **2012**, *116*, 2591– 2597.

62. Berger, G.; Soubhye, J.; van der Lee, A.; Vande Velde, C.; Wintjens, R.; Dubois, P. Clément, S.; Meyer, F. *Chempluschem* **2014**, *79*, 552–558.

63. Estarellas, C.; Frontera, A.; Quinonero, D.; Deya, P.M. *ChemPhysChem* **2011**, *12*, 2742 –2750.

64. Bauza, A.; Frontera,A. *Phys. Chem. Chem. Phys*. **2017**, *19*, 12936-12941.

65. Johnson, M. T.; Dzolic, Z.; Cetina, M.; Wendt, O. F.; Ohrstrom, L.; Rissanen, K. *Cryst. Growth Des.* **2012**, *12*, 362-368.

66. Khavasi, H. R.; Esmaeili, M. *CrystEngComm* **2014,** *16*, 8479-8485.

67. Andreev, V. P.; Ryzhakov, A. V.; Kalistratova, E. G. *Chem. Heterocycl. Comps.* **1996**, 516-518.

68. Acheson R. M.; Adcock B. *J. Chem. Soc. C* **1968**, 1045-1047.

69. Bruker Apex3 v2016.9-0, Saint V8.34A, SAINT V8.37A, Bruker AXS Inc.: Madison WI, 2016.

70. SHELXTL suite of programs, Version 6.14, Bruker AXS Inc., Madison, WI, 2000-2003.

71. Sheldrick, G. *Acta Cryst. C* **2015**, *71*, 3.

72. Hübschle, C.; Sheldrick, G.; Dittrich, B. *J. Appl. Crystallogr.* **2011**, *44*, 1281.

73. Frisch, M. J.; Trucks, G. W.; Schlegel, H. B.; Scuseria, G. E.; Robb, M. A.; Cheeseman, J. R.; Scalmani, G.; Barone, V.; Mennucci, B.; Petersson, G. A., et al. *Gaussian 09, Revision C.01*, Gaussian, Inc., Wallingford CT, 2009.

74. Zhao, Y.; Truhlar, D. *Theor. Chem. Acc.* **2008**, *120*, 215.

75. Boys, S. F.; Bernardi, F. *Mol. Phys.* **1970**, *19*, 553−566.

For Table of Contents Use Only

Title: **Effects of supramolecular architecture on halogen bonding between diiodine and heteroaromatic *N*-oxides**

Authors: *Yakov P. Nizhnik, Alex Sons, Matthias Zeller, Sergiy V. Rosokha,**

TOC graphic

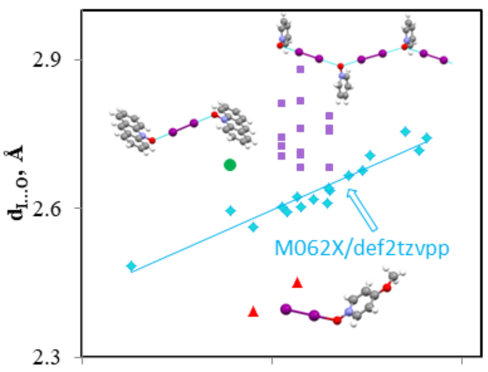

X-ray structural characterization of co-crystals of the original halogen bond donor, diiodine, with heteroaromatic *N*-oxides demonstrated that I…O separations in their 1:1 adducts are about 0.3 Å shorter than that in the 2:1 associates or in the infinite chains, and these variations are related largely to the distinct effects of halogen-bond competition in different supramolecular associates.